

Proposal of Site Theory

H. Itofuji

Ube Steel Co., Ltd.
Ube City, Yamaguchi, JAPAN

ABSTRACT

A new theory on the nucleation and growth mechanism of spheroidal, compacted/vermicular (C/V) and chunky graphite in liquid iron treated with Mg spheroidizer is proposed in this paper. The theory is based on many experimental data, such as the microstructure of specimens quenched into water during the solidification, the element maps in the microstructure of solidified specimens, scanning electron microscopy (SEM) photographs and diffraction patterns of some types of graphite extracted from the matrix in a series of study. The theory was named the "site theory." The site theory is the developed version of the bubble theory proposed by Yamamoto et al. According to the site theory, many phenomena in foundry operation can be understood rather easily.

INTRODUCTION

On the nucleation of spheroidal graphite (SG) in liquid iron, many theories have been reported to date. They are roughly divided into two groups. One is the heterogeneous nucleus theory,¹⁻⁹ and another is the bubble theory.¹⁰⁻¹⁶ Other than these two theories, the homogeneous nucleus theory¹⁷⁻²⁰ has been proposed by some researchers, but due to lack of experimental verification, no serious attention has been paid to this theory.

The heterogeneous nucleus theory claims that SG nucleates on the heterogeneous nuclei, which may be sulfide, oxide, nitride and/or carbide of Mg, Ca or rare earth elements. This idea is quite popular in not only the nucleation of SG but also that of other crystal grain. This theory is not, however, sufficient to explain the nucleation of SG because of the following reasons: Although some graphite nodules have nuclei-like objects at their center, it is quite difficult to show that such nuclei exist in all the SG. It is also difficult to imagine that they work for the nucleation of SG and continue to affect the final morphology with the spheroidal form and the polycrystal substructure. Furthermore, this theory cannot explain the phenomenon that SG forms in pure Ni-C and Fe-C-Si alloy without addition of any spheroidizer elements, when the liquid alloys are rapidly solidified.²¹

The bubble theory was first proposed by Gorschkov et al.,¹⁰ and other researchers^{11,12,14} followed. At that time, the bubble theory was hardly known among metallurgists because it only implied that the gas bubble was related to the nucleation of SG, and gave no other detailed explanation. However, the bubble theory was considerably progressed by Yamamoto, Kawano, Chang et al.^{13,15,16} The latest bubble theory is summarized as follows:

1. Graphite nucleates on the wall of a vaporized Mg and Ca gas bubble because of the free surface.
2. In rare earth elements, the adsorbed hydrogen is the resource of a gas bubble.
3. The fading phenomenon is caused by the loss of a gas bubble.
4. Spheroidal graphite can also be obtained by any other gas bubbles.
5. The gas bubble guarantees the initial form of SG.

On the growth mechanism of SG, a great number of theories have been reported, to date. In the recent theories, however, these are roughly classified into two groups. The first one is the dislocation theory,²²⁻⁴² and the another is the bubble theory.^{13,15,16}

In the last decade, the most popular theory has been the dislocation theory. The dislocation theory claims that SG is formed as the result of the spiral growth by screw dislocation, when liquid iron is treated by Mg, Ca and rare earth elements. This may be the reason that the surface of SG looked like the spiral end when its section and surface were observed by SEM. This was confirmed further by the SEM observation of the growth end of CV and chunky graphite, for the same reason as SG. The proposal of screw dislocation mechanisms is based on the following reasons:

1. Nuclei contained spheroidizer element.^{28,33}
2. Activation of melt-graphite interface by adsorption of spheroidizer elements on the prism face of graphite crystal.^{34,38}
3. Undercooling of melt by spheroidizer elements.^{39,40}
4. Change of the growth velocity on the a-axis and c-axis in the graphite crystal by amount of spheroidizer elements and by solidification rate.⁴¹

However, the spiral substructure on spheroidal, CV, or chunky graphite has not yet been verified experimentally. The screw dislocation is a common defect in graphite crystal,⁴³⁻⁴⁶ regardless of the growth process. Furthermore, the SG is obtainable without addition of any spheroidizer elements.^{13,15,16} This leads to the assumption that the spiral growth enhanced by spheroidizer is unnecessary to grow spheroidal graphite.

In the bubble theory, the growth of SG is based on the natural growth behavior of graphite crystal structure. The growth mechanism under the bubble theory can be summarized as follows:

1. Graphite centripetally grows into sphere graphite in a gas bubble.
2. After sphere graphite is surrounded by austenite shell, sphere graphite grows outward and into general SG.
3. Spheroidal graphite has a polycrystalline structure and consists of many thin plates. Each plate's face is the basal plane. The dominant growth direction is along the a-axis.

They have not, however, succeeded to verify the evidence of Mg relating to SG by the analytical method and the detail substructure. Nothing was claimed on the nucleation and growth mechanism of CV and chunky graphite. Three types of graphite must be explained by the single theory, because the same spheroidizer is used.

In solid iron, it seems that a void is very important for the nucleation and growth of temper graphite, just like the gas bubble in liquid iron. It is generally known, at present, that temper graphite nucleates and grows at the void defect in solid iron. The morphology of temper graphite depends on the shape of such defects. The defects may be itemized as follows:

1. Void.⁴⁷
2. Crack in cementite.⁴⁸
3. Phase interface between cementite and matrix.⁴⁹⁻⁵²
4. Phase interface between an inclusion and matrix.^{53,54}
5. Grain boundary.⁵⁵
6. Interface between insert material and matrix.⁵⁶
7. Joint interface of diffusionally-bonded SG iron.⁵⁷
8. Free surface on white iron⁵⁸ and on thin plate of carbon steel.⁵⁹

If the void's shape could be controlled, the morphology of temper graphite would be controlled. Lee⁶⁰ has succeeded in getting a void to be spheroidal in shape by heat treatment. Similar phenomena have been reported by Hanawa et al.⁶¹ in powder metallurgy products of Fe-Si-C and Ni-C systems. Kawano et al.⁶² have reported that the eutectic graphite can be granulated by cyclic heat treatment.

It can be considered that a spheroidal void in solid iron and a gas bubble in liquid iron are similar sites for the nucleation and growth of SG. There is no difference between these free surfaces for the nucleation and growth of SG. From this point of view, it is predicted that the morphology of not only SG but also all other types of graphite in Mg-treated irons is determined by the morphology of the void or any interfaces on the site where the graphite nucleates and grows.

In this paper, a new theory is proposed, shown by experimental evidence, that can explain a wider range of phenomena on the graphite spheroidization than can the bubble theory.

FUNDAMENTAL BEHAVIOR OF MAGNESIUM IN IRON⁷⁵

When Mg spheroidizer is added into liquid iron, temperature gradient arises from the center toward the surface. With such temperature gradient, the Mg state changes from solid to liquid and, further, to gas. The generation of Mg vapor occurs on the surface over approximately 1100C (2122F). This type of vaporization behavior is referred to as the local type in the surface boiling mode.⁶³ The formation mechanism of an Mg gas bubble in liquid iron by vaporization behavior is illustrated in Fig. 1. After the discharge of the Mg gas bubble, the vapor generation stops for a while, because liquid iron contacting with the Mg spheroidizer may locally reduce the temperature by the latent heat. The next nucleation of the Mg gas bubble may occur again, when the liquid iron regains the temperature.

The cycle of the nucleation and the discharge of the Mg gas bubble may be repeated until all the liquid Mg is consumed. The cycle speed, therefore, depends on the temperature of the base liquid iron. Since Mg has almost no solubility in liquid iron under atmospheric pressure,⁶⁴ most of the vapor gas may stay as a gas bubble.

The size of an Mg gas bubble in liquid iron can be calculated by:

$$P(\text{Mg}) = P_a + \rho gh + 2\gamma/r \quad (1)$$

- where $P(\text{Mg}) = \text{Mg vapor pressure (g/cm}^2)$
 $[\log P(\text{Mg}) = -1.299 \times 10^4/T + 4.958]$ ⁶⁵
 $T = \text{spheroidizing temperature (rankine scale)}$
 $P_a = \text{atmospheric pressure (1 atm = } 1.013 \times 10^6 \text{ dyn/cm}^2)$
 $\rho = \text{density of liquid iron (6.7 g/cm}^3)$ ⁶⁶⁻⁶⁸
 $g = \text{gravitational acceleration (980 cm/sec}^2)$
 $h = \text{depth of liquid iron (cm)}$
 $\gamma = \text{surface tension of liquid iron (1350 dyn/cm}^2 \text{ at 1355C (2607F))}$ ^{66,69-71}
 $r = \text{bubble radius (cm)}$

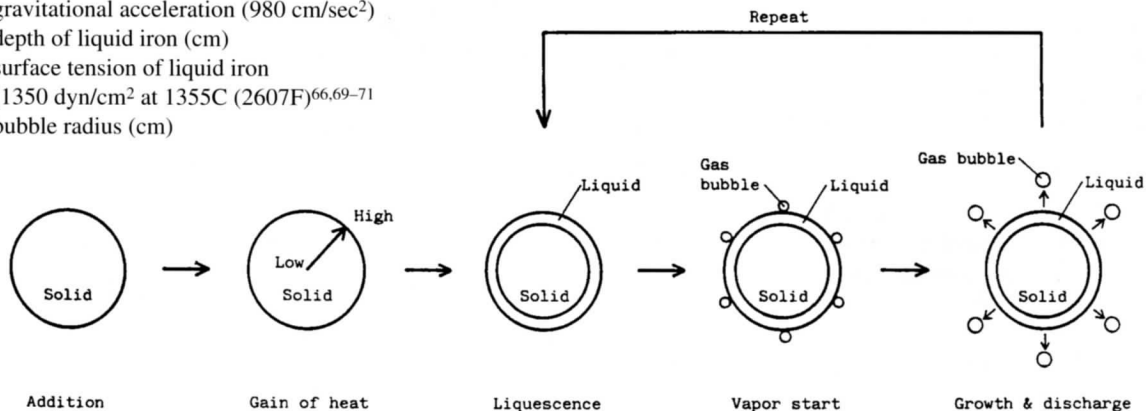


Fig. 1. Formation mechanism of an Mg gas bubble in liquid iron.

If liquid iron were treated with Mg spheroidizer at 1450C (2787F) and the depth of liquid iron was 1–100 cm, the diameter of an Mg gas bubble would be 6 μm . According to Stoke's equation, this size of Mg gas bubble floats at the ratio of approximately 10 cm/hour, as calculated through:

$$U = 2r^2 / 9\eta \cdot (\rho_o - \rho) \cdot g \quad (2)$$

- where $U = \text{floating rate of bubble in liquid iron (cm/sec)}$
 $r = \text{bubble radius (cm)}$
 $\eta = \text{viscosity of liquid iron (0.05 g/cm-sec}^2)$
 $\rho_o = \text{density of liquid iron (6.7 g/cm}^3)$
 $\rho = \text{density of bubble (= 0 g/cm}^3)$
 $g = \text{gravitational acceleration (980 cm/sec}^2)$

Then, the Mg gas bubble can suspend for 0.1–10 hours in liquid iron. If the liquid iron temperature near spheroidizer intermittently went down from 1450C (2787F), the diameter of an Mg gas bubble would be larger than 6 μm . For example, the average bubble diameter would be 19 μm at 1300C (2502F). This value is nearly equal to the size observed by Yamamoto et al.¹³ Then, the floating rate and the suspension time would be 100 cm/hour and 0.01–1 hour, respectively, in 1–100 cm depth liquid iron. The calculated floating rate and the suspension time well reflect the fading phenomena of Mg,⁷³ in practice.

The dispersion of an Mg gas bubble in liquid iron is conducted by forced-stirring during spheroidizing treatment and by self-stirring from the convection of liquid iron. In the case of forced-stirring, the liquid iron is stirred by the tapping stream. In practice, stirring is the necessary condition for good spheroidizing treatment, in any case. On the other hand, in self-stirring, liquid iron is stirred by the bubbling effect of the Mg gas bubble, a similar phenomenon to Ar bubbling for other liquid metals.

Thus, it is possible to form, suspend and disperse Mg gas bubbles in liquid iron. Graphite may dominantly nucleate onto the wall because of the free surface.

NUCLEATION AND GROWTH OF GRAPHITE^{74,75}

The nucleation and growth behavior of graphite in Mg-treated liquid iron were observed, using optical microscopy. The specimens were quenched into a water bath from the liquid state, directly, and at the selected points during the solidification. Sphere graphite under 10 μm directly precipitates in liquid iron without an austenite shell, though the final morphology is spheroidal, CV and/or chunky graphite structure. The example is shown in Fig. 2. The size of sphere graphite well matches the calculated value (<10 μm) of an Mg gas bubble in former sections.

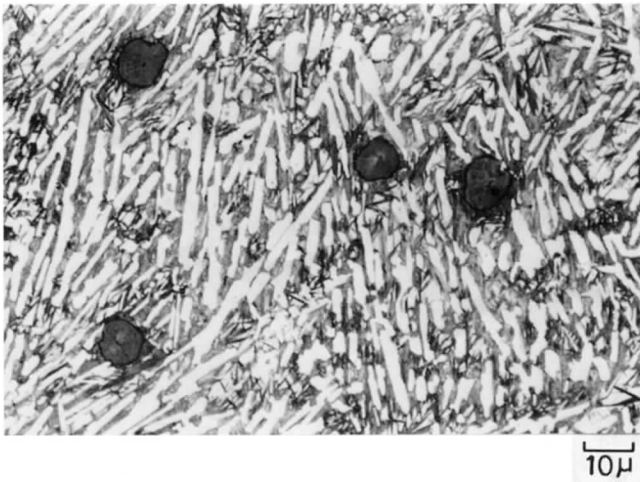
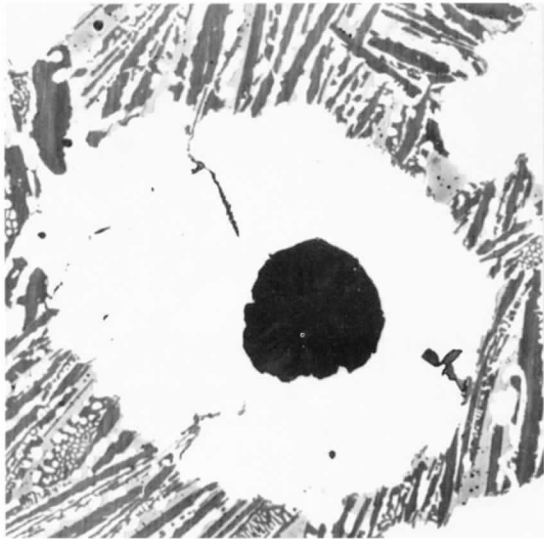
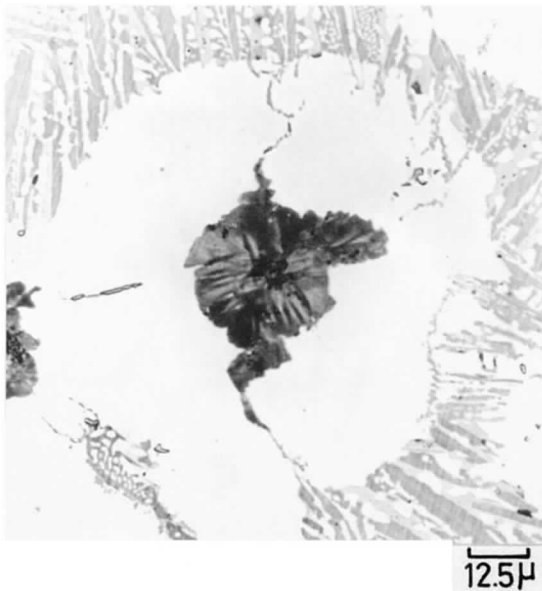


Fig. 2. Microstructure of specimen quenched at about 1350C (2462F) (c-solution etch¹⁶).



(3a)



(3b)

Fig. 3. Comparison of eutectic austenite shells during growth of general and degenerated SG (c-solution etch¹⁶).

After sphere graphite is surrounded with austenite shell, it grows into spheroidal and/or CV graphite, depending on the condition of liquid channel.⁷⁵ If sphere graphite were isolated from residual liquid iron, it would grow into SG (Fig. 3). If sphere graphite were in contact with residual liquid iron through liquid channel, it would grow into CV graphite (Fig. 4). On the other hand, chunky graphite has no direct relation to sphere graphite. When SG stops the growth, chunky graphite newly nucleates at an inclusion-austenite interface around austenite shell and austenite dendrite (Fig. 5). This is why the nodule number is too small and the nodule diameter is too big to grow larger during solidification.

These phenomena suggest that the graphite morphology depends on the site where graphite nucleates and grows. The nucleation and growth process of spheroidal, CV and chunky graphite is schematically illustrated in Fig. 6.

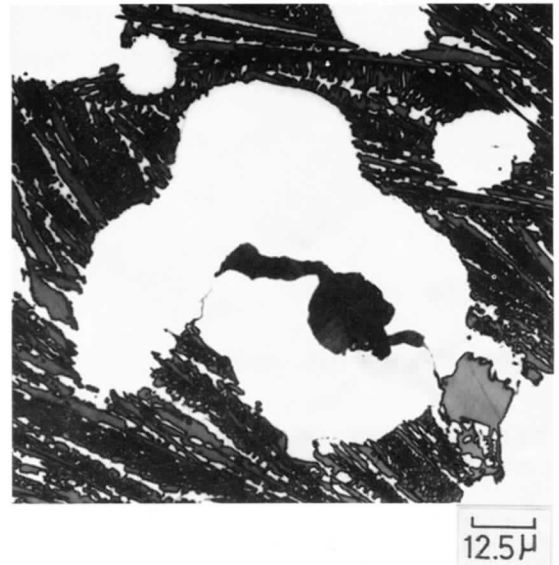


Fig. 4. CV graphite growing from sphere graphite and connected to residual liquid iron through thin liquid channel during growth (c-solution etch¹⁶).

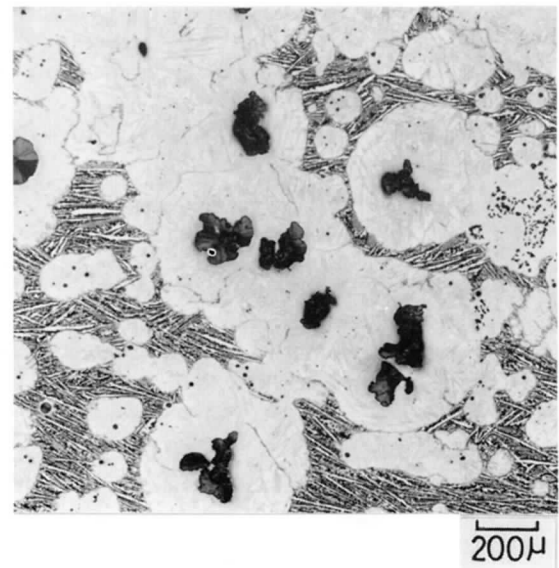


Fig. 5. Early stage of nucleation and growth of chunky graphite in quenched specimen (5% picral etch); nucleation at inclusion-austenite interface.

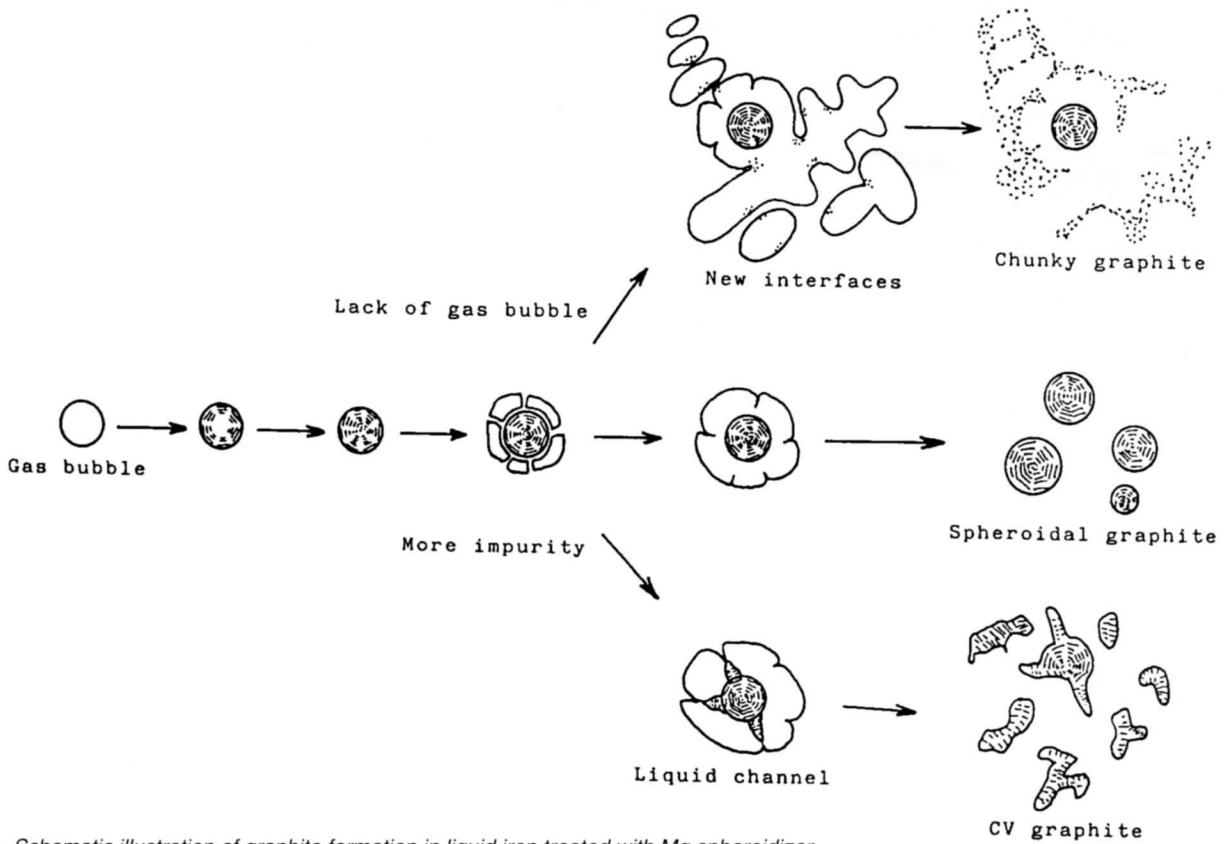


Fig. 6. Schematic illustration of graphite formation in liquid iron treated with Mg spheroidizer.

DIRECT OBSERVATION OF MAGNESIUM RELATING TO SPHEROIDIZATION^{76,77}

According to the fundamental characteristic of Mg in the liquid and solid state, it was expected that there was an Mg-rich layer around every SG. The direct observation of Mg was, therefore, tried using electron probe micro analyzer (EPMA) in conjunction with a colored mapping display system. As expected, Mg was prominent around the perimeter of every graphite nodule, resembling the halo present in a total solar eclipse. The Mg map is shown in Fig. 7. Some graphite nodules contained inclusions consisting of an Mg oxide system. However, those graphite nodules were also surrounded by the Mg halo. Most inclusions were observed at the ferrite grain boundaries, especially in the region among the old austenite skeleton. This area equates to the region where it solidifies at a late stage of the eutectic solidification.

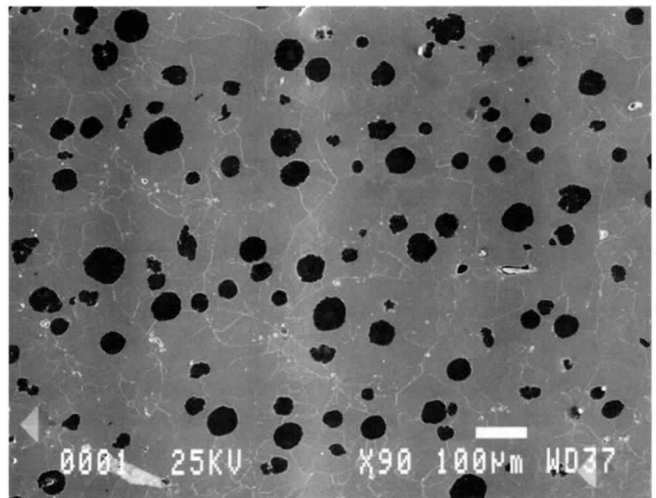
This suggests that inclusions do not influence the nucleation of SG during the early stage of solidification, because the present sites of most inclusions equated to the latter stage of solidification. It is thought that such an inclusion becomes trapped in an Mg gas bubble, and graphite subsequently precipitates in the same bubble. As a result, if there were many inclusions present in Mg-treated liquid iron, there would be more cases where inclusions were attracted to Mg gas bubbles and, as a consequence, entrapped in the graphite nodules.

As is generally known, Si has a strong relation to the nucleation and growth of SG. Every graphite nodule existed in an Si-rich region, as shown in Fig. 7. It is certain that graphite predominantly nucleates and grows onto the wall of an Mg gas bubble in the Si-rich region. It is natural for a high nodule count to have a great number of Mg gas bubbles in such an Si-rich region. The region is introduced into liquid iron by inoculation.

SUBSTRUCTURE OF GRAPHITE HISTORY^{76,78}

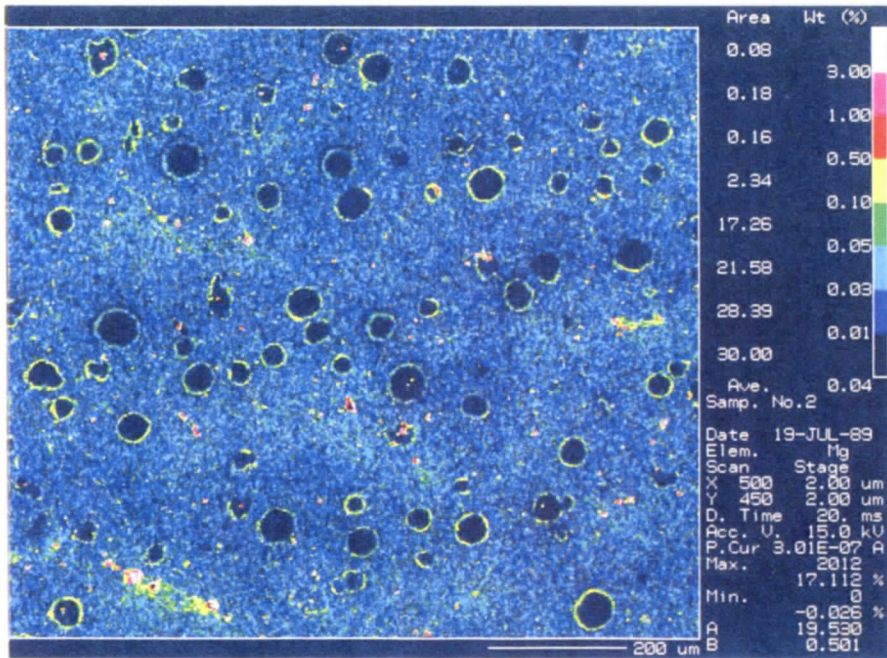
The eutectic cells of spheroidal, CV and chunky graphite were electrolytically extracted from irons. Each type of extracted graphite was observed using SEM with a high resolving ability. The SEM photos are shown in Figs. 8–10.

The spheroidal, CV and chunky graphite appear different from each other, but their substructure was basically the same. They were similarly constructed by the piling up of thin graphite plates. Each plate's face was parallel to the surface. The diffraction pattern measured with scanning transmission electron microscopy (STEM)

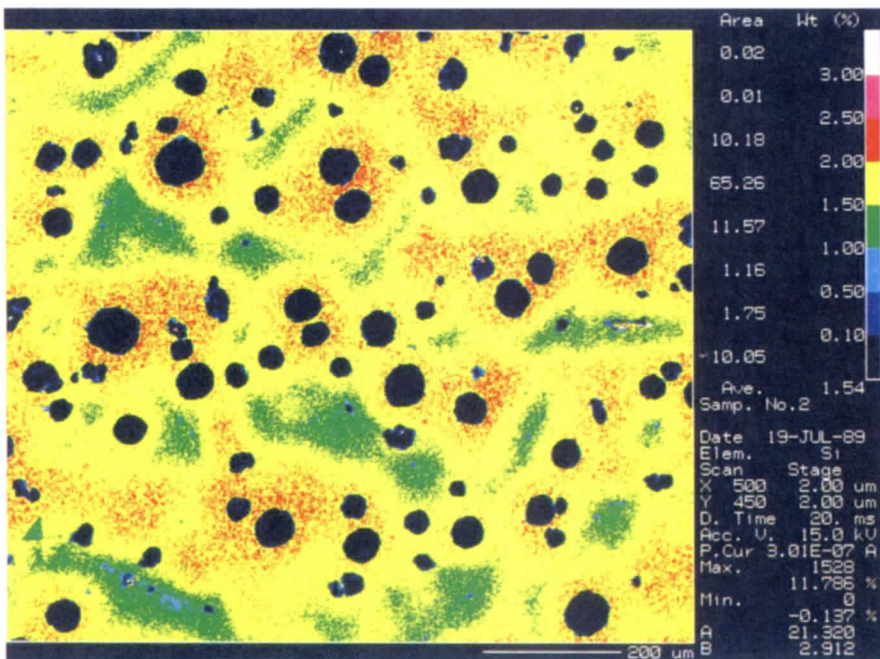


(7a) optical microstructure (3% Nital etch)

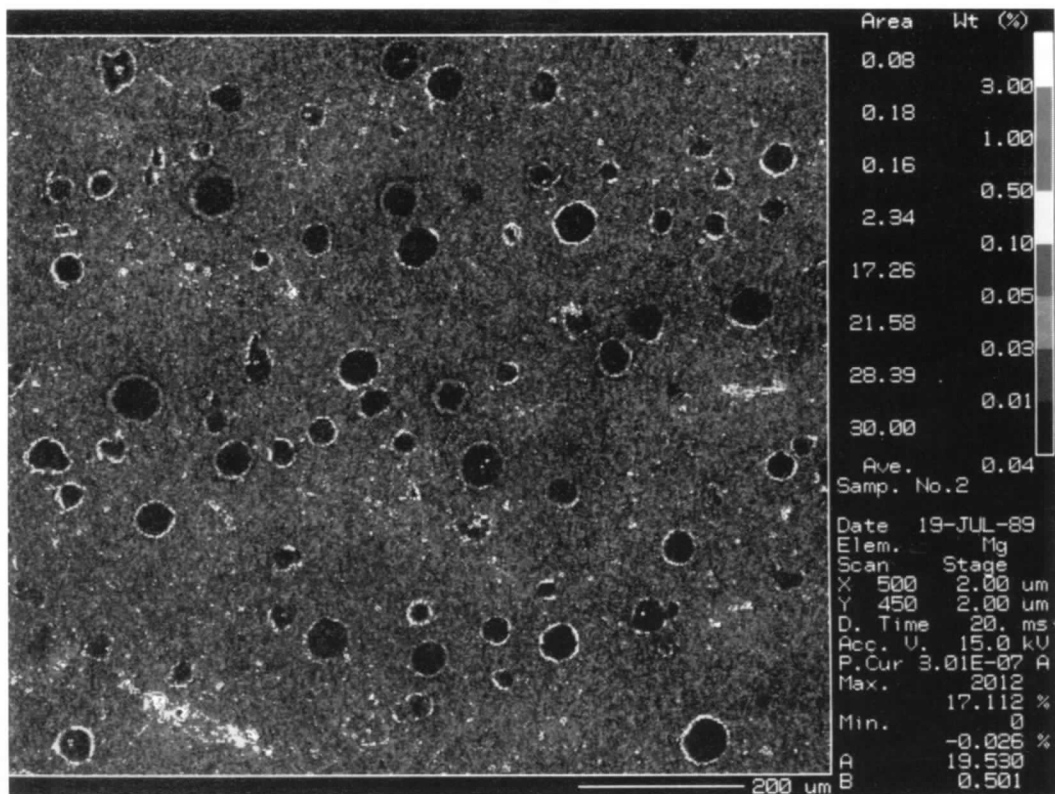
Fig. 7. Result of colored mapping analysis on SG structure.



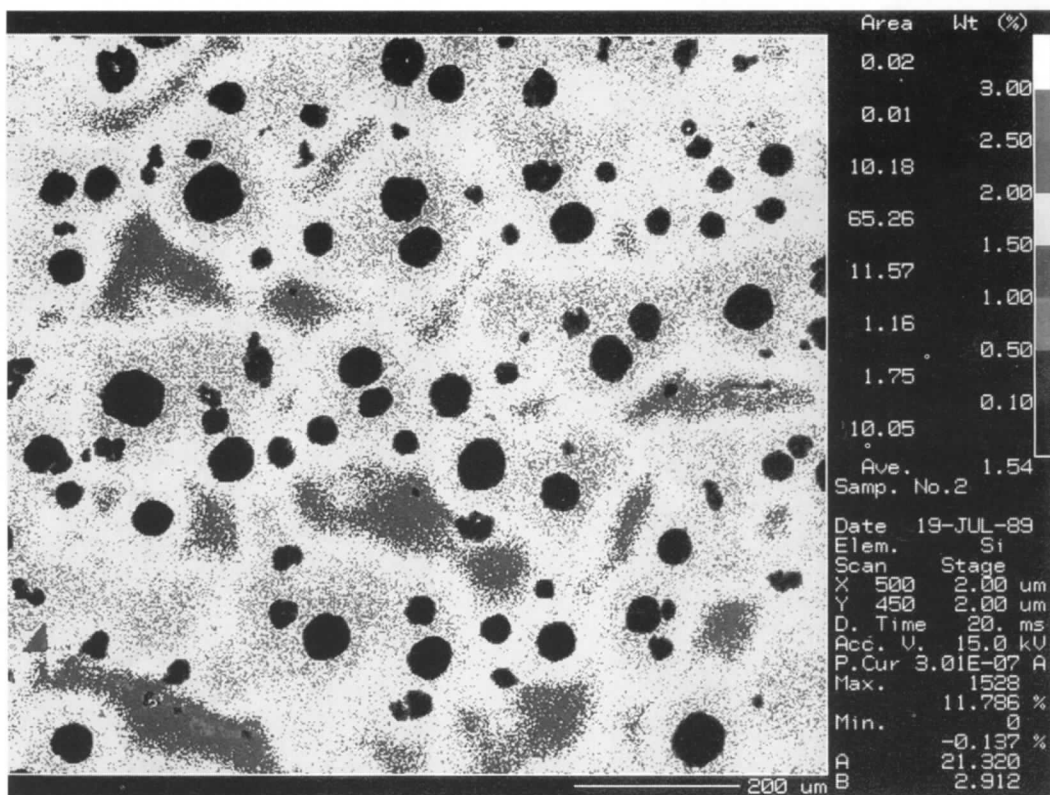
(7b) Mg map



(7c) Si map



(7b) Mg map



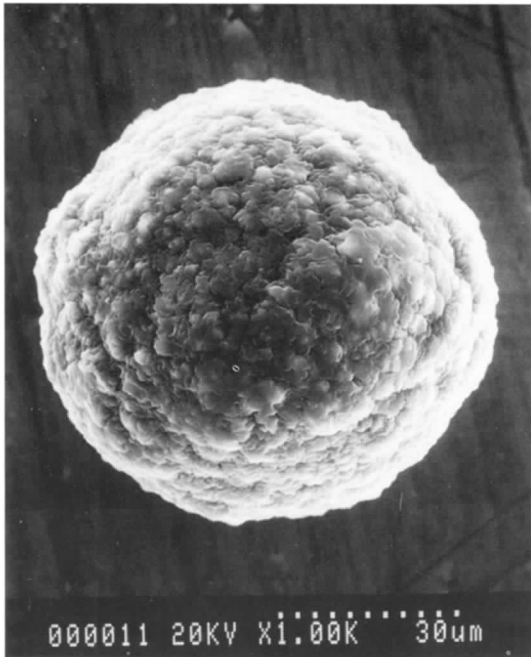
(7c) Si map

showed that such plate's face was the basal plane of the graphite crystal. This means that the natural growth behavior was never changed by other factors and was kept along the a-axis of the hexagonal graphite crystal structure.

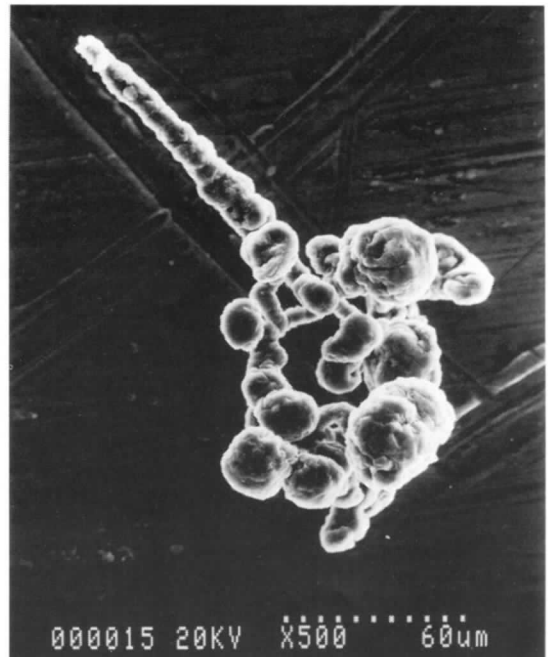
The substructure was also verified another way. Each type of extracted graphite was easily disintegrated into a single plate, block with plates, etc., without any breakage, using ultrasonic vibration

force. No other behavior, such as spiral growth, was observed. Examples of a disintegrated graphite plate are shown in Fig. 11.

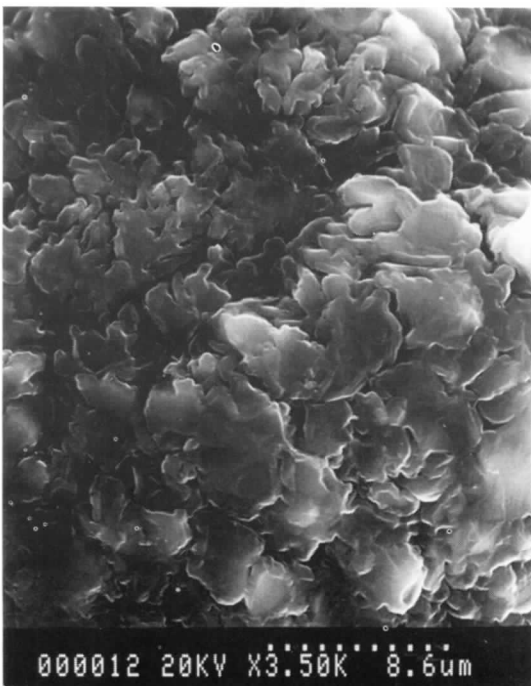
It is considered that spheroidal, CV and chunky graphite take the same behavior on the nucleation and growth in a similar vessel-like site. Otherwise, they cannot have basically the same substructure. The nucleation and growth behavior of graphite in an Mg gas bubble are shown in Fig. 12.



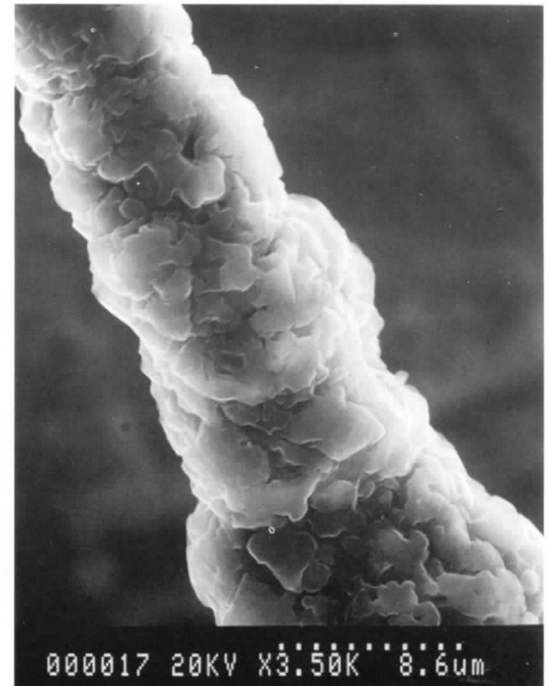
(8a) whole cell



(9a) whole cell



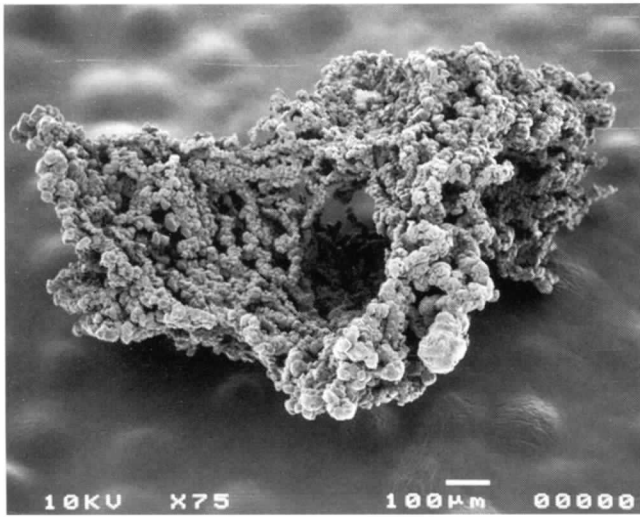
(8b) high magnification of SEM



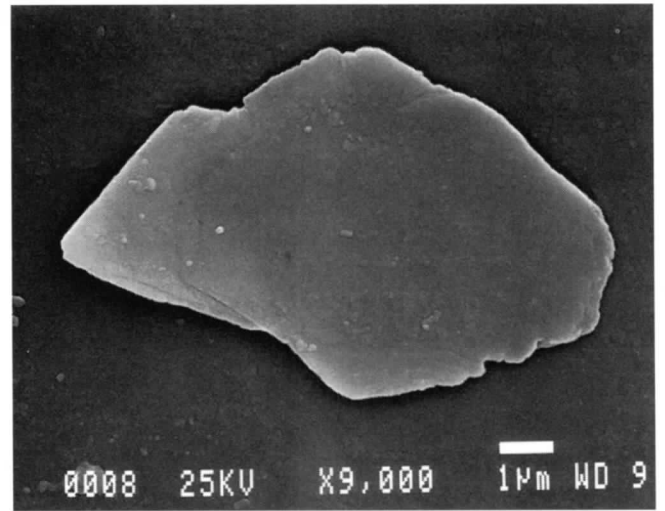
(9b) high magnification of SEM

Fig. 8. SEM structure of extracted SG cell.

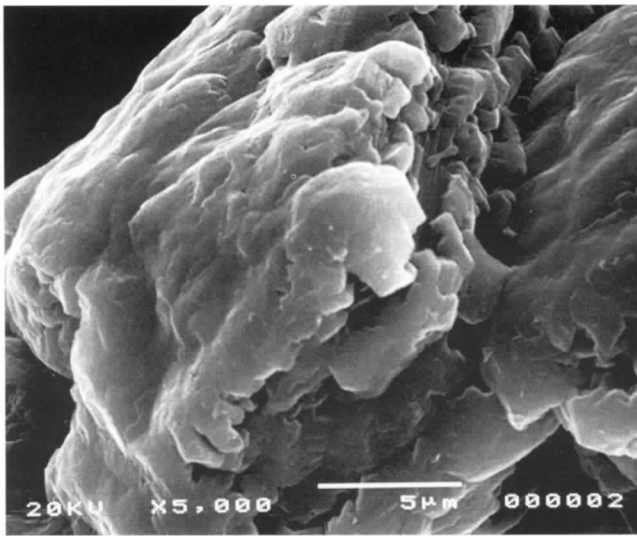
Fig. 9. SEM structure of extracted CV graphite cell.



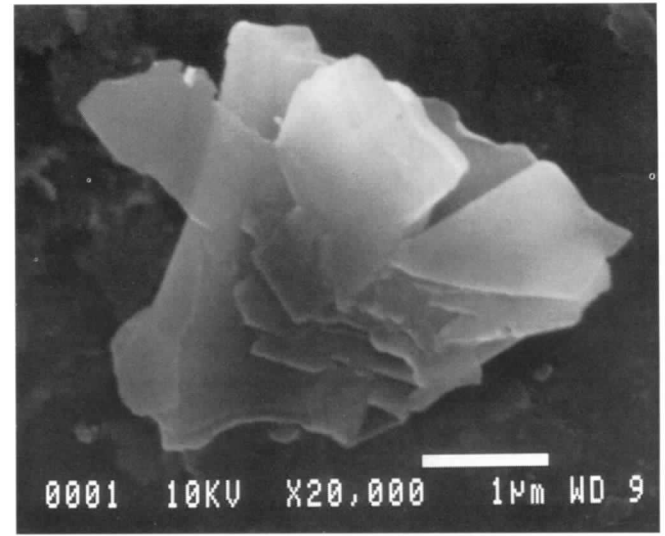
(10a) whole cell



(11a) single plate



(10b) high magnification of SEM



(11b) block

Fig. 10. SEM structure of chunky graphite cell.

Fig. 11. SEM structure of SG decomposed into single graphite plate and block of graphite plates by ultrasonic vibration force.

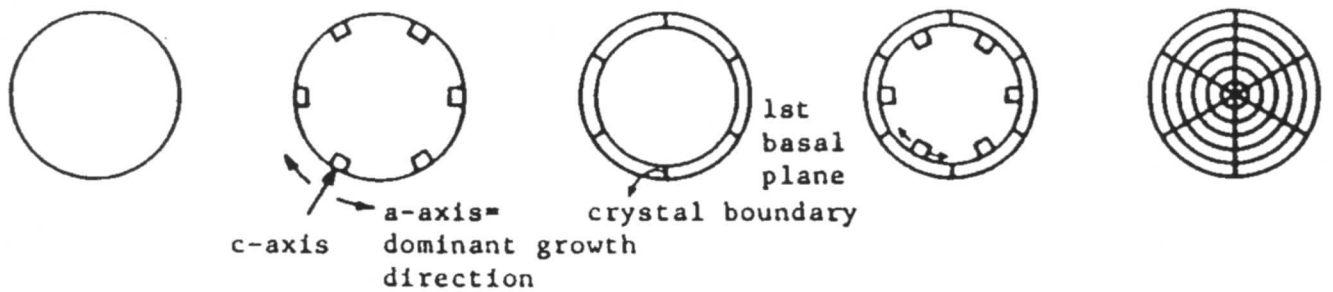


Fig. 12. Nucleation and growth mechanism of graphite in a gas bubble.

PROPOSAL OF THE SITE THEORY

A theory discussed in the Introduction was verified showing many experimental evidences. It is clear that every graphite morphology formed in Mg-treated liquid irons depends on the site where each type of graphite nucleates and grows. On their growth, the natural growth behavior of the hexagonal graphite crystal structure is never changed by other factors. The theory can be also applied to other types of graphite in liquid and solid state. Hence, this theory is named as the site theory.

Application of the Site Theory

According to the site theory, it is very important to keep the following three items in liquid iron, before and during the solidification:

1. Enough Mg gas bubbles
2. High Si segregation
3. Less impurity

Calcium and cerium turn into impurities in the case of heavy-section ductile cast iron, because they form inclusions and cause the precipitation of chunky graphite. The key point is to know what is happening in the micro-area of liquid iron.

ACKNOWLEDGMENTS

The author would like to acknowledge Y. Kawano, H. Shingu, S. Yamamoto and N. Inoyama of Kyoto University for their comments on this study. The author would also like to acknowledge H. Yamada of Ube Steel Co., Ltd. for his cooperation.

REFERENCES

1. W. Deuchler, "Spectrographic and X-ray Investigation of Isolated Graphite Spheroids in Cast Iron with Spheroidal Graphite," *Giesserei*, vol 42, Fe. (1955), P58.
2. A.P. Von Rosenstiel and H. Bakkerus, "On the Proof of Nuclei in Cast Iron with Spheroidal Graphite," *Giesserei Techn.-wiss. Beih.*, vol 16 (1964), P149.
3. R.J. Warrick, "Spheroidal Graphite Nuclei in Rare Earth and Magnesium-Inoculated Irons," *AFS Transactions*, vol 74 (1966), P722.
4. J.S. Prasad and W.C. Phelps, "A Study of the Solidification of Iron Carbon-Silicon Alloys," *Modern Casting*, vol 50, No. 6 (1966), P155.
5. M.H. Jacobs, T.J. Law, D.A. Melford and M.J. Stowel, "Basic Processes Controlling the Nucleation of Graphite Nodules in Chill Cast Iron," *Metals Technology*, (Nov 1974), P490.
6. J. Pirs and N. Mardesich, "Some Results of Investigations of the Interphase Boundary Segregations in Pearlitic and Ferritic Nodular Cast Irons," *Microstructural Science*, vol 6, No. 6 (1978), P161.
7. L.S. Ivakhnenko, "Role of Adsorption of Impure Elements on Nucleation Process of Graphite Inclusion in Cast Irons," *Litinoe Proizvodstvo*, No. 3 (1979), P2.
8. H. Fidos, "Structural Analysis of a Graphite Nodule and Surrounding Halo in Ductile Iron," *AFS International Cast Metals J.*, (Mar 1982), P54.
9. T. Kusakawa, "Observation of the Nucleus in Spheroidal Graphite of Cast Iron," *116th Grand Lecture Meeting of the Japan Foundrymen's Society*, (Oct 7-8 1989), P69.
10. A.A. Gorshkov, "On Formation Mechanism of Spheroidal Graphite," *Lit. Proizv.*, No. 3 (1955), P17.
11. H.H. Stadelmaier, "Uber Spharolithenbildung in Metallschmelzen," *Z. Metallkde.*, vol 51, No. 10 (1960), P601.
12. F.M. Levshin, "Formation of Nodular Graphite in Gray Iron," *Russ. Cast. Prod.*, (Dec 1963), P331.
13. S. Yamamoto, B. Chang, Y. Kawano, R. Ozaki and Y. Murakami, "Producing Spheroidal Graphite Cast Iron by Suspension of Gas Bubbles in Melts," *AFS Transactions*, vol 83 (1975), P217.
14. S.I. Karsay, *Ductile Iron Production I*, Quebec Iron and Titanium Corp. Publish (1976), P13.
15. S. Yamamoto, B. Chang, Y. Kawano, R. Ozaki and Y. Murakami, "Mechanism of Nodularization of Graphite on Cast Irons Treated with Magnesium," *Metal Science*, vol 12, (May 1978), P239.
16. B. Chang, K. Akechi and K. Hanawa, *Spheroidal Graphite Cast Iron: Basis, Theory, Practice*, Agne Co., Ltd. Publishing (1984).
17. A. Wittmoser, "On the Formation of Nodular Graphite in Gray Iron," *Giesserei*, vol 38 (1951), P469.
18. A.L. De Sy, "Graphite Spherulite Formation and Growth," *Foundry*, vol 81, (Nov 1953), P100.
19. H. Morrogh and W.J. Williams, "The Production of Nodular Graphite Structures in Cast Iron," *J. Iron and Steel Inst.*, vol 158 (1949), P306.
20. M. Maruyama, "Inoculation to the Vacuum-melted Iron," *IMONO*, vol 33 (1961), P266.
21. S. Banerjee, "A Review of the Formation of Spheroidal Graphite in Cast Iron," *British Foundryman*, vol 58, (Sep 1965), P344.
22. W.K. Burton, N. Cabrera and F.C. Frank, "The Growth of Crystals and the Equilibrium Structure of Their Surface," *Phil. Trans.*, A243 (1951), P299.
23. M. Hillert and Y. Lindblom, "The Growth of Nodular Graphite," *J. Iron and Steel Inst.*, vol 176 (1954), P388.
24. F.C. Frank, *Growth and Perfection of Crystals (Int. Conf. Reports)*, John Wiley & Sons, Inc. (New York), (1958), P3.
25. P.L. Walker and B.C. Banerjee, "Topology of Kish Crystal and the Effect of Oxidation in Air," *Nature*, vol 197, (Mar 1963), P1291.
26. R.A. Sidorenko, "Dislocation Mechanism of the Growth of Spheroidal Graphite in Iron," *Fiz. Met. Metallov.*, vol 20, No. 3 (1965), P412.
27. E. Fitzner and G. Schlesinger, "Spiral and Wisker Growth in Pyrolytic Carbon," *Bar. Deutsch. Keram. Gesellsch.*, vol 43, No. 3 (1966), P209.
28. P.C. Liu, C.R. Loper, Jr., T. Kimura and H.K. Park, "Observation on the Graphite Morphology in Cast Iron," *AFS Transactions*, vol 88 (1980), P97.
29. P.C. Liu, C.R. Loper, Jr., T. Kimura and E.N. Pan, "Observation on the Graphite Morphology of Compacted Graphite Cast Iron," *AFS Transactions*, vol 89 (1981), P65.
30. C. Sy-Sen, Y. Sheng, W. Zu-Lun, C. Sy-Chen and J. Shun-Lian, "The Mechanism of Spheroidal Graphite Formation During Primary Crystallization of Cast Iron," 48th International Foundry Congress, Varna Bulgaria, (Oct 4-7 1981), Paper No. 8CN.
31. E.N. Pan, K. Ogi and C.R. Loper, Jr., "Analysis of the Solidification Process of Compacted Vermicular Graphite Cast Iron," *AFS Transactions*, vol 90 (1982), P509.
32. P.C. Liu, C.L. Li, D.H. Wu and C.R. Loper, Jr., "SEM Study of Chunky Graphite in Heavy-Section Ductile Iron," *AFS Transactions*, vol 91 (1983), P119.
33. D.M. Stefanescu, M. Martinez and I.G. Chen, "Solidification Behavior of Hypoeutectic and Eutectic Compacted Graphite Cast Irons. Chilling Tendency and Eutectic Cells," *AFS Transactions*, vol 91 (1983), P205.
34. J.Y. Su, C.T. Chow and J.F. Wallace, "Solidification Behavior of Compacted Graphite," *AFS Transactions*, vol 90 (1982), P565.
35. Y. Gan and C.R. Loper, Jr., "Observations on the Formation of Graphite in Compacted and Spheroidal Graphite Cast Irons," *AFS Transactions*, vol 91 (1983), P781.
36. S.E. Franklin and A. Stark, "Application of Secondary Ion Mass Spectrometry to Study of Graphite Morphology in Cast Iron," *Metal Science*, vol 18, (Apr 1984), P187.
37. J.P. Hrusovsky and J.F. Wallace, "Effect of Composition on Solidification of Compacted Graphite Iron," *AFS Transactions*, vol 93 (1985) P55.
38. N. Yingyi and Z. Zhu, "A Study of the Rare Earth Effect on Chunky Graphite," *The Foundryman*, (Aug 1988), P390.
39. S.V. Sabramanian, D.A.R. Kay and G.R. Purdy, "Compacted Graphite Morphology Control," *AFS Transactions*, vol 90 (1982), P589.
40. A.A. Nofal, L.A. El-Manawati and M.A. Wali, "Nucleation and Growth of C/V Graphite and Other Associated Graphite Morphologies," 56th World Foundry Congress, Dusseldorf, (May 19-23, 1989), Paper No. 21.

41. C.R. Loper, Jr., R.C. Voigt, J.R. Yang and G.X. Sun, "Use of the Scanning Electron Microscope in Studying Growth Mechanism in Cast Irons," *AFS Transactions*, vol 89 (1981), P529.
42. J.Y. Chen, D.H. Wu, P.C. Liu and C.R. Loper, Jr., "Liquid Metal Channel Formation in Compacted/Vermicular Graphite Cast Iron Solidification," *AFS Transactions*, vol 94 (1986), P537.
43. F.H. Horn, *Nature*, vol 170 (1952), P581.
44. I. Minkoff and I. Einbinder, "Dendrite Growth of Graphite from Melts," *Nature*, vol 194, (May 26, 1962), P765.
45. B. Vassiliou, E.W. Roberts and I.R. Rigby, *Nature*, vol 175 (1955), P348.
46. T. Tsuzuki and T. Komoda, *J. Phys. Soc. Japan*, vol 12, 7 (1955), P778.
47. K. Kubota and S. Yamamoto, "Kinetics of Graphitization of Cementite," *J. Japan Inst. of Metals*, vol 46 (1982), P908.
48. C. Wells, *Trans. ASM* (1938), P289.
49. Y. Kaji, "Grain Boundary Precipitation of Graphite in Cast-Iron and the Thermodynamic Properties of Austenite," *J. Japan Inst. of Metals*, vol 19 (1955), P340.
50. I. Igarashi and Y. Serita, "The Effect of Some Elements on the Chilled Structures and on Their Graphitization in Cast Iron," *IMONO*, vol 24 (1952), P1.
51. D.S. Gill and D.S. Eppelsheimer, "The Mechanism of Graphitization of Fe-C-Si Alloys," *Foundry*, (Aug 1959), P60.
52. M.C. Ashton and J.G. Magney, "High Temperature Surface Observations of White Cast Irons," *AFS Cast Metals Research J.*, vol 9, (Mar 1973), P31.
53. H. Morrogh, *J. Iron and Steel Inst.*, vol 143 (1941), P207.
54. S. Sueyoshi and K. Suenaga, "Effects of Pre-treatment on the Graphitization Behavior in Hypo-Eutectoid Low Alloy Steel," *J. Japan Inst. of Metals*, vol 42 (1978), P676.
55. S. Sueyoshi and K. Suenaga, "Effects of Alloying Elements on the Graphitization of Hypo-Eutectoid Steel," *J. Japan Inst. of Metals*, vol 43 (1979), P333.
56. N. Tsutsumi and T. Fuse, "Abnormal Structure at Molten Metal Joint Part of Spheroidal Graphite Cast Iron with Other Metallic Materials," *Trans. of Waseda University Casting Inst.*, (1983), Report No. 39.
57. H. Horie, T. Kowata and T. Okura, "Graphite Formation at the Bond Interface in Diffusion-Bonded Spheroidal Graphite Iron," *IMONO*, vol 61, No. 7 (1989), P475.
58. K.P. Bunin, *All Microstructure in Irons*, (1976), P155.
59. T. Nakamura and M. Sato, "Graphite Pollution Mechanism at the Surface of Steel Sheet on Annealing," *J. Iron and Steel Inst. of Japan*, vol 77 (1991), P1702.
60. Y. Lee, "Action of Gas and Vapor Element on Microstructural Change in Iron," Thesis for Doctor's Degree of Kyoto University (1986).
61. K. Hanawa, K. Akechi, Z. Hara and T. Nakagawa, "Nodular Graphite Formation in P/N Products from Cast Iron Swarf Powder and Fe-Si-C Mixed Powders," *Trans. Japan Inst. of Metals*, vol 21, No. 12 (1980), P765.
62. Y. Kawano and T. Sawamoto, "Production of Cast Iron with Fine Granular Graphite," *AFS Transactions*, vol 88 (1980), P463.
63. Ie I. Nesis, *Boiling of Liquid*, Publishing Hause Nauka (Moscow), (1973).
64. A.A. Nayeb-Hashemi, J.B. Clark and L.J. Swartzendruber, "The Fe-Mg System," *Bulletin of Alloy Phase Diagrams*, vol 6, No. 3 (1985), P235
65. P.K. Trojan and R.A. Flinn, "A New Method for Determination of Liquid-Liquid Equilibria as Applied to the Fe-C-Si-Mg System," *Trans. Am. Soc. Metals*, vol 54, No. 3 (1961), P549.
66. K. Loberg, "Die Oberflächspannung magnesiumfreier und magnesiumhaltiger naheutektischer Eisen-Kohlenstoff-Legierungen mit Zusätzen von Wismut, Blei, Kupfer, Titan und Zirkon und ihre Bedeutung für die Bildung von Kugelgraphit," *Giesserei techn.-wiss.*, vol 18, Heft 4 (1966), S189.
67. C.F. Walton and T.J. Opar, *Iron Casting Handbook*, Iron Casting Society, Inc. Publishing (1981), P486.
68. Japan Foundrymen's Society, *IMONO Handbook*, 4th Edition, Maruzen Co., Ltd. Publishing (1986), P4.
69. K. Grutter and B. Marincek, "The Influence of Surface Tension on the Formation of Graphite in Cast Iron," *The Engineers' Digest*, vol 16, No. 2 (1955), P69.
70. D. Pohl and E. Sheil, "Über die Oberflächenspannung von Gusseisen," *Giesserei*, vol 43, (Dec 1956), S833.
71. K. Herfurth, Untersuchungen über den Einfluss verschiedener Zusätze auf die Oberflächenspannung von flüssigem Gusseisen mit dem Ziel, Zusammenhänge zwischen der Oberflächenspannung und der Entstehung der verschiedenen Graphitformen zu finden. (Freiberg, 1963), (Dr.-Ing.-Diss., Bergakademie Freiberg.), vgl. Freib. Forsch.-H., Abt. B, Nr 105 (1966), S267.
72. *Handbook of Physical Properties for Liquid Iron and Slag*, JISI of Japan Publish (1972), P53.
73. B. Chang, S. Yamamoto, Y. Kawano and R. Ozaki, "On the Fading Behavior in Magnesium-Treated Cast Irons," *J. of the Japan Institute of Metals*, vol 41, No. 10 (1977), P1019.
74. H. Itofuji, Y. Kawano, N. Inoyama, Y. Yamamoto, B. Chang and T. Nishi, "The Formation Mechanism of Compacted/Vermicular Graphite in Cast Irons," *AFS Transactions*, vol 91 (1983), P831.
75. H. Itofuji, "Study On Graphite Spheroidization In Cast Irons," Thesis for Doctor's degree of Kyoto University (1994).
76. H. Itofuji and H. Uchikawa, "Formation Mechanism of Chunky Graphite in Heavy-section Ductile Cast Irons," *AFS Transactions*, vol. 98 (1990), P429.
77. H. Itofuji, "Magnesium Map of the Spheroidal-graphite Structure in Ductile Cast Irons," Color-printing, *Cast Metals*, vol 5, No. 1 (1992), P6/discussion, vol 5, No. 4 (1993), P235.
78. H. Itofuji, Y. Kawano, S. Yamamoto, N. Inoyama, H. Yoshida and B. Chang, "Comparison of Substructure of Compacted/Vermicular Graphite with Other Types of Graphite," *AFS Transactions*, vol 91 (1983), P313.